Hydroxamic Acid Derivatives as Potent Peptide Deformylase Inhibitors and Antibacterial Agents

Christian Apfel, David W. Banner, Daniel Bur, Michel Dietz, Takahiro Hirata, Christian Hubschwerlen,* Hans Locher, Malcolm G. P. Page, Wolfgang Pirson, Gérard Rossé,† and Jean-Luc Specklin

Preclinical Research, F. Hoffmann-La Roche Ltd., CH-4070 Basle, Switzerland

Received January 18, 2000

Low-molecular-weight β-sulfonyl- and β-sulfinylhydroxamic acid derivatives have been synthesized and found to be potent inhibitors of *Escherichia coli* peptide deformylase (PDF). Most of the compounds synthesized and tested displayed antibacterial activities that cover several pathogens found in respiratory tract infections, including *Chlamydia pneumoniae, Mycoplasma pneumoniae, Haemophilus influenzae,* and *Moraxella catarrhalis*. The potential of these compounds as antibacterial agents is discussed with respect to selectivity, intracellular concentrations in bacteria, and potential for resistance development.

Introduction

Antibiotic resistance among Gram-positive bacteria (staphylococci, enterococci, and streptococci) is becoming a major health concern. Therefore, there is an urgent need to discover antibiotics with new modes of action. The protein synthesis machinery is targeted by many successful drugs including chloramphenicol, tetracyclines, macrolides, and aminoglycosides. In this respect, peptide deformylase (PDF), an enzyme that removes the formyl group from the N-terminal methionine of nascent polypeptides, represents an interesting and unexploited target since this enzyme is conserved and believed to be essential in eubacteria[1−3] and is not required for protein synthesis in eukaryotes.

Rationale

Screening for inhibitors of *E. coli* PDF resulted in the identification of actinonin **(1)**, a natural hydroxamic acid derivative earlier described as an aminopeptidase inhibitor[4,5] and an antibacterial agent.[6] PDF is a metalloenzyme which has recently been recognized to utilize iron (Fe^{2+})[7−10] as the catalytic metal for *N*-formyl hydrolysis. The metal is coordinated to two histidine residues, one cysteine residue, and a molecule of water, which can donate a proton to Glu133 (Chart 1). The X-ray structure of the *E. coli* PDF suggests a mechanism for the deformylation of peptides.[10,11] On the basis of the structures of **1** and of the general substrates **A**, we hypothesized that the complex formed with a hydroxamic acid mimics the transition state and therefore predicted that smaller hydroxamic acid derivatives of type **B** should be PDF inhibitors.

In this paper we describe the synthesis and the evaluation of β-sulfonyl- and β-sulfinylhydroxamic acids as PDF inhibitors and antibacterial agents.

Chemistry

The 3-substituted β-lactones **3** were prepared according to literature precedent by an efficient [2+2] cycloaddition reaction of trimethylsilyl ketene to the appropriate aldehyde, R_2CHO.[12,13] The key carboxylic acid intermediates **4** were obtained by two different routes: either by 1,4-conjugated addition of thiols on β-substituted acrylic acids **2** or by CsF-catalyzed ring opening of β-lactones **3** with thiols (Scheme 1). The carboxylic acids **4** were then converted into the corresponding protected hydroxamate derivatives **5** either by reaction with *O*-benzyl- or *O*-TBDMS-protected hydroxylamines in the presence of DCC or, alternatively, by loading onto hydroxylamine-Wang resin after activation with HATU (*O*-(7-azabenzotriazol-1-yl)-*N,N,N′,N′*-tetramethyluronium hexafluorophosphate). The hydroxamates **5** were oxidized either to the corresponding sulfones **6** with Oxone or mCPBA or to sulfoxides **7** with 3-phenyl-2-(phenylsulfonyl)oxaziridine.[14] Deprotection using standard methods (Scheme 1) afforded the target sulfones **8** and sulfoxides **9** (Table 1). Separation of the two enantiomers of the *O*-benzyl hydroxamate **6d** by preparative HPLC on a chiral column gave the two enantiomers *(R)*-**8d** and *(S)*-**8d** after subsequent deprotection.

The α-hydroxy-β-sulfinylhydroxamic derivatives **15a** and **15b** were obtained starting from *trans*-2-hepten-1-ol (Scheme 2). A sequence employing a modified Sharpless epoxidation using L- or D-diethyl tartrate[15,16] followed by RuO_4 oxidation afforded the *trans*-epoxy acids **11a** (2*R*,3*S*) and **11b** (2*S*,3*R*), respectively. Further treatment of **11a** and **11b** with thiophenol in the presence of $LiClO_4$ on alumina and subsequent reaction with *O*-tetrahydropyranylhydroxylamine[17] in the presence of carbonyldiimidazole gave the sulfide derivatives **13a** and **13b**. Oxidation with 3-phenyl-2-(phenylsulfonyl)oxaziridine and final deprotection with acidic Amberlyst IR15 afforded derivatives **15a** (*2S*,3*R*) and **15b** (2*R*,3*S*) as mixture of diastereoisomers, due to the nonstereoselective oxidation of the sulfide.

Results and Discussion

1. Inhibition of the Native *E. coli* PDF. The β-sulfonylhydroxamic acid derivatives **8** were found to be potent inhibitors of the native *E. coli* PDF. The structure−activity relationship (SAR) is presented in

* To whom correspondence should be addressed. Tel: 41 61 688 5967. Fax: 41 61 688 6459. E-mail: christian.hubschwerlen@roche.com.
† Present address: Selectide Corp., A Subsidiary of Aventis Pharmaceuticals, Tucson, AZ 85737.

10.1021/jm000018k CCC: $19.00
Published on Web 05/20/2000

Chart 1. Mechanism for the Deformylation of Peptides and Rational Design of PDF Inhibitors

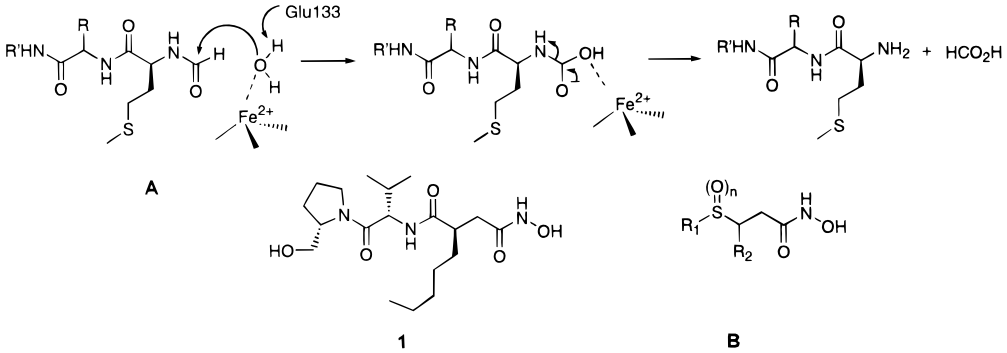

Scheme 1[a,b]

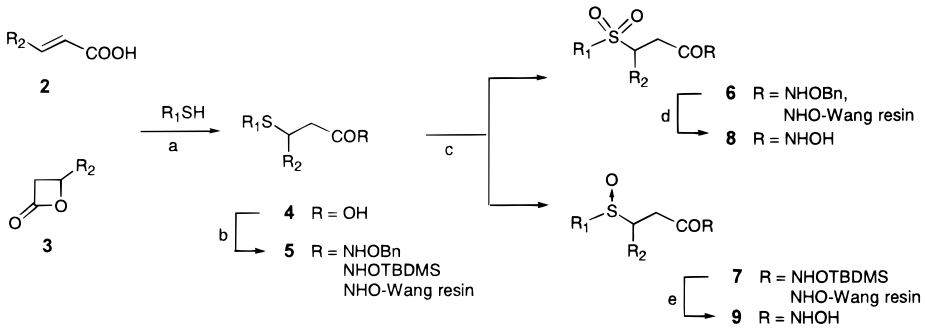

[a] Reagents: methods A−D refer to general procedures described in the Experimental Section; (a) methods A & C: **2**, DIPEA; methods B & D: **3**, CsF; (b) method A: NH_2OBn, DDC; methods B & D: NH_2O-Wang resin, HATU; method C: $NH_2OTBDMS$, DCC; (c) method A: Oxone; method B: mCPBA; methods C & D: 3-phenyl-2-(phenylsulfonyl)oxaziridine; (d) method A: H_2, Pd/C; method B: TFA; (e) method C: KF; method D: TFA. [b] R_1 and R_2 are defined in Table 1.

Scheme 2[a,b]

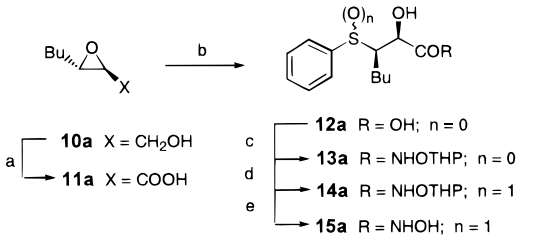

[a] Reagents: (a) RuO_4, $NaIO_4$; (b) PhSH, $LiClO_4/Al_2O_3$; (c) NH_2OTHP, CDI, HBT; (d) 3-phenyl-2-(phenylsulfonyl)oxaziridine; (e) Amberlyst IR15. [b] The enantiomeric series **10b**−**15b** was obtained using (−)-diethyl D-tartrate in the preparation of **10b**.

Table 2. The activity of these inhibitors is strongly influenced by the nature of the substituent R_2, which occupies the same position in the enzyme as the methionine side chain of the natural substrates does. Moreover, stronger inhibition was obtained with unsubstituted aromatic rings or linear aliphatic chains (propyl to pentyl). Although the maximum activity was observed with the *n*-butyl side chain (e.g. **8d**), *E. coli* PDF can also accommodate bulkier groups (e.g. **8h**). For the substituent R_1, which could, in principle, mimic the peptide backbone of the substrates, best activities were obtained with aryl groups (e.g. **8l**−**p**). The nature and the position of the substituent on the phenyl ring both played an important role in determining the affinity (compare **8m** and **8n** or **8m** and **8p**). In particular, the *N*-acetyl group in **8o** induced the lowest IC_{50} value due to further favorable contacts with the enzyme. Benzyl, cycloalkyl, and long alkyl substituents led to less potent inhibitors (e.g. **8i**−**k**).

The activity of the inhibitors is also largely dependent on the stereochemistry at the carbon in β-position to the hydroxamic acid. This is illustrated with compound **8d**, where one enantiomer turned out to be 100 times more active than the other. An X-ray crystal structure of **8d** bound to PDF was determined (Figure 1). It is clearly seen that the (*R*)-enantiomer is strongly bound in the active site, which is consistent with modeling considerations. The same configuration is found at the corresponding C(β)-position in actinonin.

The binding mode of (*R*)-**8d** (Figure 1) suggested that, since only one sulfone oxygen is involved in a hydrogen-bonding interaction and the other appears to make no participating interaction with the protein, the corresponding sulfoxide might bind just as well, or even better. Compared to the corresponding β-(arylsulfonyl)-hydroxamic acid template, the β-(arylsulfinyl)hydroxamic acid template gave slightly less potent inhibitors (compare **9a** and **8d** or **9b** and **8m**), but a similar trend in the SAR was observed in both classes. The sulfoxide functionality introduces an additional uncontrolled chiral center leading to a mixture of epimers. Modeling suggests that only one of the four isomers present in the mixture can make a good hydrogen-bonding interaction with the backbone NH of Ile44 (Figures 1 and 2). The higher IC_{50} values observed for the sulfoxides **9** are consistent with this suggestion.

Inspection of the complex of *E. coli* PDF with (*R*)-**8d** (Figure 1) indicated that only small substituents are tolerated in the α-position. As shown in Figure 2, an α(*S*)-hydroxyl substituent was predicted to make favorable interactions through two additional donor and acceptor H-bonds with residue Gly45, whereas an α(*R*)-

Table 1. Preparation of β-Sulfonyl- and β-Sulfinylhydroxamic Acids

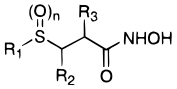

compd	R_1	R_2	R_3	n	method[a]	yield[b] (%)	elemental anal.[c]	MS (m/z)
8a	phenyl	methyl	H	2	A	45	NA	243[d]
8b	phenyl	ethyl	H	2	A	67	NA	258.0[e]
8c	phenyl	propyl	H	2	A	74	$C_{12}H_{17}NO_4S$	272.0[e]
8d	phenyl	butyl	H	2	A	82	$C_{13}H_{19}NO_4S$	286.1[e]
(*R*)-8d	phenyl	butyl	H	2	A[g]	97	NA	284.1[f]
(*S*)-8d	phenyl	butyl	H	2	A[g]	98	NA	284.1[f]
8e	phenyl	pentyl	H	2	A	63	$C_{14}H_{21}NO_4S$	300.3[e]
8f	phenyl	phenyl	H	2	A	67	$C_{15}H_{15}NO_4S$	306.2[e]
8g	phenyl	benzo[1,3]dioxol-5-yl	H	2	A	62	$C_{16}H_{15}NO_6S$	348.2[e]
8h	phenyl	2-furanyl	H	2	A	51	$C_{13}H_{13}NO_5S$	294.2[e]
8i	hexyl	butyl	H	2	A	90	$C_{13}H_{27}NO_4S$	292.3[e]
8j	cyclohexyl	butyl	H	2	A	76	$C_{13}H_{25}NO_4S$	290.3[f]
8k	benzyl	butyl	H	2	A	21	$C_{14}H_{21}NO_4S$	299[d]
8l	2-naphthyl	butyl	H	2	A	95	$C_{17}H_{21}NO_4S$	334.2[e]
8m	4-MeO-phenyl	butyl	H	2	A	79	$C_{14}H_{21}NO_5S$	314.2[e]
8n	3-MeO-phenyl	butyl	H	2	B	2	NA	314.2[c]
8o	4-AcNH-phenyl	butyl	H	2	A	88	$C_{15}H_{22}N_2O_5S$	341.2[e]
8p	4-Br-phenyl	butyl	H	2	B	10	NA	362 364[f]
9a	phenyl	butyl	H	1	C	22	$C_{13}H_{19}NO_3S$	268.3[f]
9b	4-MeO-phenyl	butyl	H	1	C	11	NA	298.4[f]
9c	3-MeO-phenyl	butyl	H	1	D	5	NA	298.3[f]
9d	2-naphthyl	butyl	H	1	C	45	NA	318.2[e]
9e	4-Br-phenyl	butyl	H	1	D	13	NA	345 347[f]
15a[h]	phenyl	butyl	OH	1	E	63	NA	284.1[f]
15b[i]	phenyl	butyl	OH	1	E	34	NA	284.1[f]

[a] Methods A−E refer to general procedures described in the Experimental Section. [b] For the final step. [c] C, H, N, S. [d] EI (M). [e] ISP $(M + H)^+$. [f] ISN $(M - H)^-$. [g] Compound obtained through HPLC separation on a chiral column. [h] (2*S*,3*R*). [i] (2*R*,3*S*).

Table 2. Inhibition of Native PDF and in Vitro Antibacterial Activity Against Selected Strains

compd	PDF-Fe[a] IC_{50} (μM)	MIC (μg/mL) *E. coli* DC2	MIC (μg/mL) *M. catarrhalis* RA21
1	0.006	1	<0.06
8a	22.00	>32	>32
8b	3.000	>64	>64
8c	0.160	64	4
8d	0.035	8	<0.25
(*R*)-8d	0.016	2	<0.25
(*S*)-8d	1.900	>128	16
8e	0.140	2	<0.06
8f	0.160	32	8
8g	1.100	16	1
8h	0.094	32	4
8i	0.530	64	4
8j	0.230	8	<0.25
8k	0.190	128	16
8l	0.023	8	0.5
8m	0.031	16	0.5
8n	0.086	16	2
8o	0.011	16	1
8p	0.120	16	2
9a	0.100	1	<0.25
9b	0.099	2	<0.25
9c	0.094	4	0.25
9d	0.064	2	<0.25
9e	0.210	1	<0.125
15a	0.280	1	<0.06
15b	7.400	32	4

[a] Inhibition of the isolated *E. coli* enzyme demonstrated to contain mainly iron (IC_{50}'s are mean values of at least 2 experiments).

hydroxyl substituent would collide with the side chain of Leu91 (Figure 1). This was confirmed by the greater potency of **15a** over **15b** in the β-sulfinyl series.

2. Inhibition of PDF from Other Organisms. PDF from *B. subtilis* and *S. pneumoniae*, used as purified recombinant native enzymes, were similarly inhibited

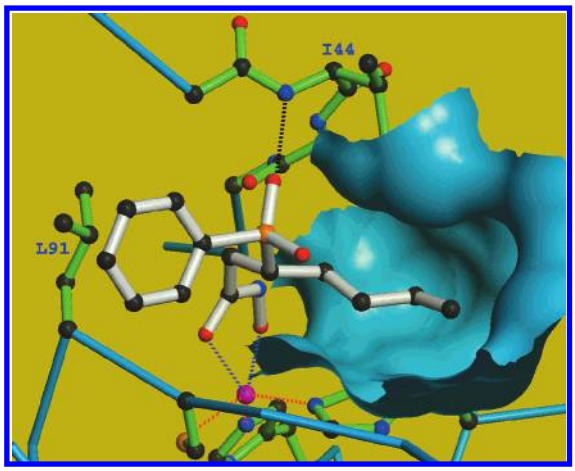

Figure 1. X-ray crystal structure of (*R*)-**8d** bound to Ni-PDF. The inhibitor is shown as ball-and-stick in white. The protein Cα trace is in blue, with selected active site residues in green. The S1′ subsite of the protein is represented as a blue surface. The Ni^{2+} ion is shown as a magenta ball, with red dashed bonds to its three protein ligands and blue dashed bonds to the two hydroxamate oxygens. The hydrogen bond from the NH of Ile44 to a sulfone oxygen is also indicated.

by these hydroxamic acids (e.g. compound **8d** with IC_{50} 0.096 and 0.34 μM, respectively, and compound **9a** with IC_{50} 0.046 and 0.24 μM, respectively).

3. Inhibition of Endoproteases. The β-sulfonyl- and β-sulfinylhydroxamic acid derivatives **8** and **9**, respectively, turned out to be highly selective for PDF over representative endopeptidases found in the cardiovascular system (Table 3). Less selectivity was observed with respect to various matrix metalloproteases (MMP-1, -13, -7, -12).[18−21] The relevance of this latter finding for the use of this class of derivatives as antibiotics remains to be evaluated, but it appears that

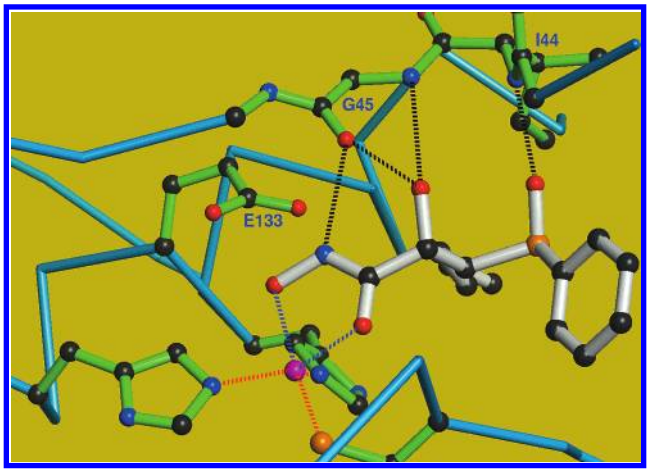

Figure 2. Model predicting the binding mode of **15a**. Color scheme as in Figure 1. The predicted hydrogen-bonding interaction with Gly45 is indicated.

Table 3. Inhibition of Several Endopeptidases and MMPs by Selected PDF Inhibitors

	IC_{50} (μM)[a]							
compd	PDF-Fe	ACE	ECE	NEP	COL-1	COL-3	MAT	HME
8d	0.035	81	>50	18	0.11	0.022	1.10	0.012
***(R)*-8d**	0.016	34	>100	2.50	0.150	0.079	2.10	0.042
***(S)*-8d**	1.9	>100	>100	15	0.300	0.018	1.20	0.009
8l	0.023	12.4	~450	0.50	0.070	0.009	1.50	0.013
8j	0.230	>100	78	1.65	0.054	0.100	0.29	0.014
9a	0.100	>100	>100	2.60	0.093	nd[b]	nd[b]	nd[b]

[a] ACE, angiotensin-converting enzyme; ECE, endothelin-converting enzyme; NEP, neutral endopeptidase; COL-1, collagenase-1 (MMP-1); COL-3, collagenase-3 (MMP-13); MAT, matrilysin (MMP-7); HME, human macrophage elastase (MMP-12). [b] nd, not determined.

this cross-reactivity would not be prohibitive for short-term treatment. In addition, the opportunities for more selective inhibitors are still not fully exploited. The structural differences between the substrate recognition sites of PDF and MMPs appear to allow the design and synthesis of more selective inhibitors.

4. Antibacterial Activity in Vitro. The PDF inhibitors were routinely tested for antibacterial activity with the permeable outer membrane mutant *E. coli* DC2 and the pathogen *M. catarrhalis* RA21. Antibacterial activity was observed for most compounds. This was especially the case for the most potent enzyme inhibitors (Table 2). However, there was not a good correlation between the IC_{50} values and the minimum inhibitory concentrations (MIC). For example, compounds having long linear R_2 side chains (compare **8e** and **8c**) showed better antibacterial activity than expected. We propose this may be related to the greater lipophilicity of the molecule, connected with better permeation of the bacterial membrane. β-Sulfinylhydroxamic acid derivatives were found to be consistently more potent against bacteria than their corresponding β-sulfonyl derivatives despite the stronger enzyme inhibition observed in the latter series. The β-sulfinylhydroxamic acid derivative **9a** and its corresponding β-sulfonyl derivative **8d** were further characterized as representative examples. The antibacterial spectrum of these compounds is presented in Table 4. Activity against the major pathogens *S. aureus*, *E. coli*, and *S. pneumoniae* was observed albeit at relatively high concentrations. In contrast, chemotherapeutically relevant activity was observed against *C. pneumoniae*, *M. pneumoniae*, *H. influenzae*, and *M. catarrhalis*.

5. Uptake of Inhibitors 8d and 9a in *E. coli*. Several lines of evidence indicate that antibacterial activity is indeed related to inhibition of the peptide deformylase.[22] Nevertheless, the antibacterial activity is generally lower than expected from the strong enzyme inhibition. Therefore the intracellular uptake of radiolabeled **8d** and **9a** was studied in *E. coli* (Figure 3). Both compounds were rapidly taken up into the strain DC2, which has a mutation in lipopolysaccharide (LPS), allowing the outer membrane to become more permeable.[23,24] An equilibrium concentration was established within 3 min. The steady-state level reached was only about one-fourth of that expected for equilibration. Addition of the uncoupler CCCP (carbonyl cyanide *m*-chlorophenyl hydrazone) at equilibrium clearly increased the steady-state level of accumulation (Figure 3, open symbols). Using the parental strain, *E. coli* UB1005, the accumulation was even lower, with a value approximately 6-fold less than the equilibrium level (Figure 3). The lower accumulation strongly indicates that the outer membrane acts as a barrier for the penetration of these compounds. Furthermore, the effect of CCCP suggests the existence of an active efflux system. We assume that both effects contribute to the low intracellular concentration. Similar results were obtained when the uptake under conditions close to the ones used for in vitro antibacterial activity tests (presence of Iso-Sensitest broth (Oxoid); data not shown) was measured.

The sulfoxide **9a** showed 8−16 times higher antimicrobial activity than the sulfone **8d** against *E. coli* DC2. However, the intracellular concentration of both compounds in *E. coli* DC2 was about 10 ng/mg dry weight of cells at 100 μM of the external concentration. Thus the higher antimicrobial activity of **9a** compared to **8d** could not be explained by different uptake and must be related to other factors.

6. In Vitro Resistance Development in *E. coli*. The development of resistance was tested in vitro in *E. coli* with **9a** and found to occur in high frequency.[22] Resistance development in *S. aureus* against actinonin was also reported recently.[25] Resistant mutants had a slow growth phenotype as has been found in transformylase/deformylase double knock-out mutants. This indicates the presence of an escape mechanism, probably through formylation independent initiation, as is the case in eukaryotes.[3]

Conclusion

Potent inhibition of bacterial PDF has been achieved with low-molecular-weight hydroxamic acid derivatives that were designed and synthesized based on the discovery of actinonin in screening for inhibitors of *E. coli* PDF. The β-(arylsulfonyl)- and β-(arylsulfinyl)-hydroxamic acids **8** and **9** displayed useful antibacterial activity. The sulfoxide **9a** and the sulfone **8d** were further characterized as representative examples of these classes, and their antibacterial spectra cover some interesting pathogens found in respiratory tract infections such as *C. pneumoniae*, *H. influenzae*, *M. pneumoniae*, and *M. catarrhalis*. However, the development of resistance toward these antibiotics in vitro[22,25] as well

Table 4. In Vitro Antibacterial Activity of Selected Inhibitors of PDF Against Different Species

bacteria	MIC (μg/mL)			
	erythromycin	**1**	**8d**	**9a**
Escherichia coli ATCC 25922	>64	64	128 (128)[a]	32
Escherichia coli DC2[b]	4	2	8 (2)	0.5
Pseudomonas aeruginosa ATCC 27853	>64	>128	>128 (>128)	>128
Stenotrophomonas maltophilia 1AC739	32	16	4	<0.25
Moraxella catarrhalis RA21	<0.125	0.125	<0.25 (<0.25)	0.06
Haemophilus influenzae 11	2	2	4 (2)	1
Mycoplasma pneumoniae ATCC 29342	<0.06	>64	1 (0.5)	0.25
Chlamydia pneumoniae AR-39	0.06	4	0.5 (0.5)	0.25
Staphylococcus aureus ATCC 25923	0.25	32	256 (128)	16
Enterococcus faecalis ATCC 29212	2	>128	>128	>128
Enterococcus faecium vanA E25_1	>64	>128	>128	>128
Bacillus subtilis ATCC 585969	<0.125	8	1 (1)	0.25
Streptococcus pneumoniae ATCC 49619	<0.125	32	128 (128)	32
Streptococcus pneumoniae 1/1[c]	>64	128	128	64

[a] Values in parentheses refer to the (*R*)-**8d** enantiomer. [b] Outer membrane permeable mutant. [c] Penicillin-resistant.

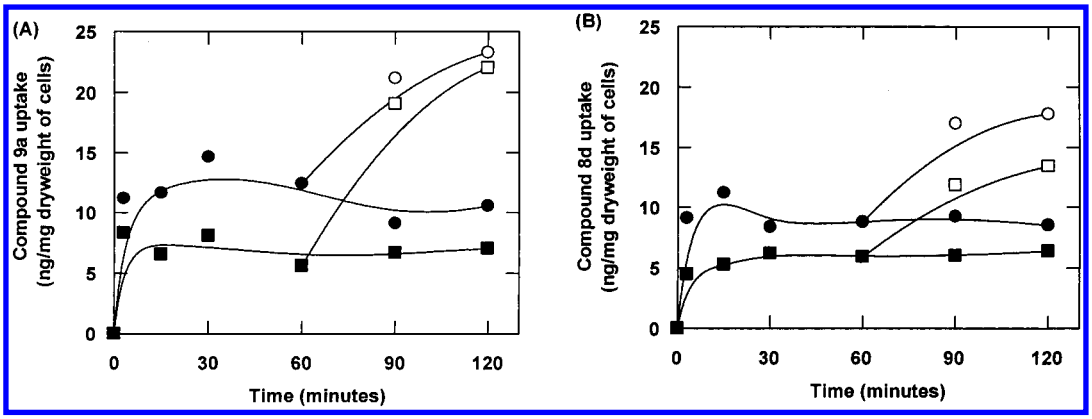

Figure 3. Uptake of hydroxamic acid derivatives in *E. coli*. Uptake of 100 μM each of (A) 3-[^{14}C]-radiolabeled **9a** or (B) 3-[^{14}C]-radiolabeled **8d**, in *E. coli* DC2 (outer membrane permeable mutant) (●) or *E. coli* UB1005 (wild type) (■). Open symbols indicated the uptake after 100 μM CCCP was added at 60 min, in DC2 (○) and UB1005 (□).

as a recent report[26] stating that not all bacteria require the formylation pathway poses some questions as to the validity of PDF as target for broad-spectrum antibacterial chemotherapy.

The low intracellular inhibitor concentrations observed in bacteria are certainly another disadvantage for broad chemotherapeutic application of the described hydroxamic acid derivatives. It remains to be seen if PDF inhibition is a valid approach for the development of antibacterials.

Experimental Section

General. Solvents were dried by filtration through Al_2O_3 (neutral, Brockmann no. 1) when necessary and stored over a bed of molecular sieves (3 Å). Hydroxylamine-Wang resin (200−400 mesh, 1.04 mmol/g) was purchased from Bachem. All organic solutions obtained after extraction were worked up by washing with H_2O and brine, dried over $MgSO_4$ and evaporated under reduced pressure with a H_2O bath temperature below 35 °C. Chromatography was performed using Merck silica gel 60 (particle size 40−63 μm). Chiral separation was performed on a 250-4 Chiralpak AD column (solvent EtOH/*n*-hexane, 6:4). TLC was performed on Merck TLC plates (silica gel 60 F_{254}) and the plates were visualized with Cl_2 and a solution of *o*-toluidine. Proton NMR spectra were recorded on a Bruker FT AC-250 (250 MHz) spectrophotometer in DMSO-d_6 solution (unless indicated otherwise). Chemical shifts (δ) are reported in ppm relative to Me_4Si as internal standard. Coupling constants (*J*) are given in Hz. IR spectra were recorded on a Nicolet FT IR 20 SXB. Ion spray and EI mass spectra were measured on a Finnigan MAT SSQ 7000 and Perkin-Elmer Siex API III recorder, respectively. Elemental analyses are indicated by the symbol of the elements; analytical results were within 0.4% of the theoretical values.

Abbreviations: DIPEA, *N*-ethyldiisopropylamine; DCE, dichloroethane; NMP, *N*-methylpyrrolidinone.

Method A: (*RS*)-3-(Phenylsulfonyl)heptanoic Acid Hydroxyamide (8d). (a) (*RS*)-3-(Phenylsulfanyl)heptanoic Acid Benzyloxyamide (5d; R_1 = Ph; R_2 = Bu; R = NHOBn). A solution of 2-heptenoic acid (650 mg; 5.0 mmol), PhSH (0.55 mL; 5.3 mmol) and DIPEA (0.96 mL; 5.5 mmol) in DMF (5 mL) was stirred at 60 °C for 48 h. The DMF was evaporated under reduced pressure and the residue, dissolved in CH_2Cl_2 (20 mL), was reacted with $BnONH_2$ (855 mg; 5.3 mmol), 1-hydroxybenzotriazole (766 mg, 5.0 mmol) and DCC (1.04 g; 5.0 mmol). After stirring overnight, the solution was diluted with CH_2Cl_2 and washed with 1% $NaHCO_3$ (10 mL), worked up and chromatographed (AcOEt/*n*-hexane) affording 1.2 g of a yellow oil (70%). ^{1}H NMR: 0.83 (t, J = 6, 3H); 1.2−1.6 (m, 6H); 2.23 (2dd, J = 15 and 6, 2H); 3.50 (m, 1H); 4.78 (s, 2H); 7.38 (s, 10H); 11.1 (s, 1H).

(b) (*RS*)-3-(Phenylsulfonyl)heptanoic Acid Benzyloxyamide (6d). A solution of **5d** (1.2 g; 3.5 mmol) in acetone (75 mL) was treated dropwise with a solution of Oxone (3.8 g; 6.3 mmol) in H_2O (25 mL) and stirred overnight at room temperature. The acetone was evaporated under reduced pressure and the aqueous layer was extracted twice with AcOEt. The combined organic layers were worked up and chromatographed (AcOEt/*n*-hexane, 2:1) affording 0.86 g of a colorless oil (65%). IR (KBr): 1654, 1446, 1304, 1148 cm^{-1}. ^{1}H NMR: 0.77 (t, J = 6, 3H); 1.2−1.5 (m, 5H); 1.70 (m, 1H); 2.20 (dd, J = 7.5 and 15, 1H); 2.50 (dd, J = 6 and 15, 1H); 3.5 (m, 1H); 4.72 (s, 2H); 7.6−7.9 (m, 5H); 11.20 (s, 1H).

(c) (*RS*)-3-(Phenylsulfonyl)heptanoic Acid Hydroxyamide (8d). A solution of **6d** (375 mg; 1 mmol) in MeOH (15 mL) was hydrogenated over 10% Pd/C (100 mg). After stirring

for 2 h, the reaction mixture was diluted with CH_2Cl_2 and the catalyst was filtered off. The filtrate was evaporated under reduced pressure and the residue was crystallized from CH_2Cl_2/hexane. The solid was purified by chromatography (CH_2Cl_2/MeOH, 9:1) affording 234 mg (82%) of colorless material. IR (film): 1666, 1447, 1303 cm^{-1}. ^1H NMR: 0.76 (t, $J = 6$, 3H); 1.2−1.5 (m, 5H); 1.75 (m, 1H); 2.2 (dd, $J = 8$ and 15, 1H); 2.45 (dd, $J = 6$ and 15, 1H); 3.57 (m, 1H); 7.8−7.95 (m, 5H); 8.95 (s, 1H); 10.61 (s, 1H).

Method B: (*RS*)-3-(4-Bromobenzenesulfonyl)heptanoic Acid Hydroxyamide (8p). (a) 4-Butyloxetan-2-one (3; R_2 = Bu). A solution of trimethylsilyl ketene (6.4 g; 55 mmol) in CH_2Cl_2 (20 mL) was added dropwise at −20 °C to a solution of valeraldehyde (4.3 g; 50 mmol) and 0.5 M BF_3·Et_2O solution (1 mL) in CH_2Cl_2 (40 mL). After stirring at 0 °C for 1 h, 2 drops of H_2O was added and the mixture was further stirred at room temperature. The solvent was evaporated under reduced pressure and the residue, dissolved in CH_3CN (30 mL), was further treated with KF hydrate (1 g). The mixture was stirred for 2 h, the solid filtered off and the filtrate evaporated. The residue was purified by chromatography (hexane/CH_2Cl_2/AcOEt, 8:1:1) leaving 3.4 g (53%) of colorless oil. ^1H NMR: 0.93 (t, $J = 6$, 3H); 1.34−1.47 (m, 6H); 1.74−1.9 (m, 2H); 3.05 (dd, $J = 5$ and 18, 1H); 3.51 (dd, $J = 5$ and 18, 1H); 4.46−4.55 (m, 1H).

(b) 3-Butyl-3-(4-bromophenylsulfanyl)propionic Acid (4p). 4-Bromothiophenol (0.41 g; 2.2 mmol) was added to a suspension of CsF (0.34 g; 2.2 mmol) in DMF (4 mL). The suspension was stirred for 10 min, then treated with **3p** (0.14 g; 1.1 mmol). The reaction was stirred overnight then filtered and evaporated. The residue was purified by chromatography (CH_2Cl_2/MeOH, 95:5) affording 0.29 g (83%) of pale yellow oil. MS (ISN): 315; 317 $(M - H)^-$. ^1H NMR: 0.83 (t, $J = 6$, 3H); 1.18−1.7 (m, 6H); 2.38−2.62 (m, 2H); 3.36−3.50 (m, 1H); 7.36−7.36 (d, $J = 8$, 2H); 7.52−7.56 (d, $J = 8$, 2H); 12.4 (b, 1H).

(c) Loading on a Hydroxylamine-Wang Resin. Hydroxylamine-Wang resin (250 mg; 0.25 mmol, 1% cross-linking, 38−75 μM, 1 mmol/g) was swollen with DMA (5 mL). A solution of **4p** (120 mg; 0.38 mmol) in DMA (0.4 mL), was treated with a 0.5 N solution of HATU (0.7 mL; 0.38 mmol) in NMP and with a 1.5 N solution of DIPEA (0.7 mL; 1.13 mmol) in NMP. After 5 min of shaking at room temperature, the solution was added to the hydroxylamine-Wang resin. The reaction mixture was shaken for 2 h, filtered off, and washed with DMA (3 × 4 mL) and with isopropyl alcohol (3 × 3 mL). This resin was used directly in the next reaction step. ATR (attenuated total reflection) FTIR: 1670 cm^{-1}.

(d) Oxidation with mCPBA. The above-described resin (0.25 mmol) was washed with DCE (3 × 4 mL) and then treated with a 0.25 M solution of mCPBA (4.0 mL; 1.0 mmol) in CH_2Cl_2. The reaction mixture was shaken for 3 h, filtered off, and washed with DCE (3 × 4 mL), isopropyl alcohol (3 × 3 mL) and DCE (3 × 4 mL). This resin was used directly in the next reaction step.

(e) (*RS*)-3-(4-Bromobenzenesulfonyl)heptanoic Acid Hydroxyamide (8p). The above-described resin was treated with a solution of TFA/H_2O/CH_2Cl_2 (4 mL; 70:2:28). The reaction mixture was shaken for 3 h, filtered off and washed with TFA/H_2O/CH_2Cl_2 (2 mL; 70:2:28). The combined eluates were evaporated. The residue was purified by preparative HPLC (YMC Pack Pro C_{18} column, 5 μm, 120 Å, 50 × 20 mm; H_2O/CH_3CN gradient) yielding 14 mg (10%) of solid.

Method C: Mixture of (*RS*)- and (*SR*)-3-[(*RS*)-Benzenesulfinyl]heptanoic Acid Hydroxyamide (9a). (a) (*RS*)-3-(Phenylsulfanyl)heptanoic Acid (*tert*-Butyldimethylsilyl)hydroxyamide (5d′; R_1 = Ph, R_2 = Bu, R = NHOTBDMS). A solution of *trans*-2-heptenoic acid (796 mg; 6 mmol), PhSH (793 mg; 7 mmol) and DIPEA (1.54 mL; 9 mmol) in DMF (10 mL) was stirred at 100 °C for 48 h. The DMF was evaporated, and the residue, dissolved in CH_2Cl_2 (20 mL), was treated with NH_2O-TBDMS (1.06 g; 7.2 mmol) and DCC (1.56 g; 7 mmol). The solution was stirred for 4 h then treated with Fuller's earth (0.5 g) and the resulting suspension stirred for 30 min and filtered. The filtrate was concentrated and the residue was purified by chromatography (AcOEt/*n*-hexane) affording 1.8 g of light brown material (81%). MS (ISN): 366.2 $(M - H)^-$. IR (film): 1659, 1529, 1256, 835 cm^{-1}. ^1H NMR: −0.06 and 0 (2s, 2 × 3H); 0.7−1.6 (m, 18H); 2.12 (d, $J = 6$, 2H); 3.4 (m, 1H); 7.3 (m, 5H); 10.6 (s, 1H).

(b) Mixture of (*RS*)- and (*SR*)-3-[(*RS*)-Benzenesulfinyl]heptanoic Acid Hydroxyamide (9a). A solution of **5d′** (1.8 g; 5 mmol) in CH_2Cl_2 (50 mL) was treated with 3-phenyl-2-(phenylsulfonyl)oxaziridine (1.34 g; 51 mmol). The resulting suspension was stirred for 2 h then evaporated to dryness under reduced pressure. The residue was purified by chromatography (AcOEt/hexane, 1:1) affording 290 mg of colorless solid (22%). Mp: 138 °C. MS (ISN): 268.3 $(M - H)^-$. IR (film): 1668, 1635, 11468, 1443, 1017 cm^{-1}. ^1H NMR: 0.87 (t, $J = 7$, 3H); 1.2−1.75 (m, 6H); 1.85 (dd, $J = 6$ and 15; 1H); 2.1 (dd, $J = 8$ and 15, 1H); 3.0 (m, 1H); 7.6 (m, 5H); 8.8 (s, 1H); 10.5 (br, 1H).

Method D: (*RS*)- and (*SR*)-3-[(*RS*)-4-Bromobenzenesulfinyl]heptanoic Acid Hydroxyamide (9e). (a) Oxidation with 2-(Phenylsulfonyl)-3-phenyloxaziridine. The resin (0.25 mmol) obtained in step 3 of method B was washed with DCE (3 × 4 mL) and treated with a 0.25 M solution of 2-(phenylsulfonyl)-3-phenyloxaziridine (2.6 mL; 0.28 mmol) in CH_2Cl_2. The reaction mixture was shaken for 10 h and filtered. The resin was sequentially washed with DCE (3 × 4 mL), isopropyl alcohol (3 × 3 mL) and DCE (3 × 4 mL). This was used directly in the next step.

(b) (*RS*)- and (*SR*)-3-[(*RS*)-4-Bromobenzenesulfinyl]heptanoic Acid Hydroxyamide (9e). The above-described resin was treated as in the preparation of **8p** (method B). The crude product was purified by preparative HPLC to give 12 mg (13%) of **9e**. MS (ISN): 345.2 and 347.2 $(M - H)^-$. ^1H NMR: 10.4 (s, 1H, NH); 8.76 (s, 1H, OH); 7.76 (d, $J = 8$, 2H); 7.54 (d, $J = 8$, 2H); 2.99−3.10 (m, 1H); 1.98−2.18 (m, 2H); 1.12−1.48 (m, 6H); 0.84 (t, $J = 7$, 3H).

Method E: 1:1 Mixture of (*2S,3R*)-3-[(*R*)- and (*S*)-Benzenesulfinyl]-2-hydroxyheptanoic Acid Hydroxyamide (15a). (a) (*2S,3S*)-(3-Butyloxiranyl)methyl Alcohol (10a). A solution of tetraisopropyl orthotitanate (1.85 mL) in CH_2Cl_2 (300 mL) was cooled to −25 °C and treated sequentially with 6 g of powered, activated molecular sieves (4 Å) and 1.43 mL of (+)-diethyl l-tartrate. The solution was further stirred for 15 min then treated with 45 mL of a 5 M solution of *t*-BuO_2H in CH_2Cl_2. The resulting solution was stirred for 30 min at this temperature then treated dropwise with a solution of *trans*-2-hepten-1-ol (12 g) in CH_2Cl_2 (40 mL). The reaction was stirred at −20 °C overnight and quenched by addition of H_2O (60 mL). The mixture was further stirred at −24 °C for 30 min, then treated with a 30% NaOH solution (7 mL; saturated with salt). The organic layer was worked up and evaporated to leave a colorless oil. The excess of *t*-BuO_2H was eliminated by azeotropic distillation with toluene. The residue was purified by chromatography (AcOEt/hexane, 3:7) and crystallization from *n*-hexane at −20 °C. ^1H NMR ($CDCl_3$): 0.91 (t, $J = 6$, 3H); 1.3−1.8 (m, 6H); 2.9 (m, 2H); 3.63 (m, 1H); 3.89 (m, 1H). $[\alpha]_D$ −33° (MeOH; *c* 1). (2*R*,3*R*)-enantiomer **10b**: $[\alpha]_D$ +32° (MeOH; *c* 1).

(b) (*2R,3S*)-3-Butyloxirane-2-carboxylic Acid (11a). A solution of **10a** (9.5 g; 73 mmol) in a mixture of CH_2Cl_2/CH_3CN/H_2O (450 mL; 1:1:2.5) was treated sequentially with RuO_2 (122 mg; 0.073 mmol) and $NaIO_4$ (63 g; 294 mmol) while the pH was kept at 4.5 by addition of 2 N NaOH solution then 1 N $NaHCO_3$ solution by automatic titration. After stirring for 24 h, $NaIO_4$ (31 g; 144 mmol) was added and the reaction was further stirred. The pH of the reaction was brought to 8.5 by addition of saturated Na_2CO_3 solution and the reaction mixture was diluted with CH_2Cl_2 (400 mL). The organic layer was separated and washed with H_2O (100 mL). The combined aqueous layers were acidified to pH 2 with 6 N H_2SO_4 at 0 °C and extracted with CH_2Cl_2 (3 × 200 mL). The organic layer was worked up to leave 3 g (28%) of colorless liquid. MS (ISN): 143.2 $(M - H)^-$. ^1H NMR ($CDCl_3$): 0.92 (t, $J = 6$, 3H); 1.3−1.75 (m, 6H); 3.20 (dt, $J = 2$ and 6, 1H); 3.26 (d, $J = 2$,

1H); 10.0 (b, 1H). $[\alpha]_D$ −19° ($CHCl_3$; *c* 1). (2*S*,3*R*)-enantiomer **11b**: $[\alpha]_D$ +26° ($CHCl_3$; *c* 1).

(c) (*2S,3R*)-2-Hydroxy-3-(phenylsulfanyl)heptanoic Acid (12a). A suspension of $LiClO_4/Al_2O_3$ (2 mmol/g; 6 g; 12 mmol) in CH_2Cl_2 was treated with PhSH (1.32 g; 12 mmol) and stirred at room temperature for 30 min. The resulting suspension was treated with **11a** (0.86 g; 6 mmol) and the resulting mixture was further stirred overnight. The mixture was filtered and evaporated. The residue was purified by chromatography (CH_2Cl_2/MeOH, 9:1) affording 430 mg (28%) of colorless gum. $_1$H NMR: 0.82 (t, *J* = 6, 3H); 1.2−1.7 (m, 6H); 3.4 (m, 1H); 4.02 (m, 1H); 7.40 (m, 5H).

(d) (*2S,3R*)-2-Hydroxy-3-(phenylsulfanyl)heptanoic Acid (Tetrahydropyran-2-yloxy)amide (13a). A solution of 1,1′-carbonyldiimidazole (331 mg; 2 mmol) and 1-hydroxybenzotriazole (276 mg; 2 mmol) in CH_3CN (10 mL) was sequentially treated with **12a** (432 mg; 17 mmol) and after 30 min NH_2-O-THP (220 mg; 19 mmol). The mixture was then heated under reflux overnight. The reaction mixture was evaporated under reduced pressure and the residue was redissolved in CH_2Cl_2. The organic layer was washed with $NaHCO_3$, and further worked up and chromatographed (*n*-hexane/AcOEt, 2:1) leaving 110 mg (18%) of colorless oil. ^{1}H NMR: 0.85 (t, *J* = 6, 3H); 0.75−1.75 (m, 12H); 3.45 and 4.05 (2m, 2 × 1H); 4.90 (m, 1H); 6.0 (d, *J* = 6, 1H); 7.2−7.5 (m, 5H); 11.05 (2s, 1H).

(e) (*2S,3R*)-3-Benzenesulfinyl-2-hydroxyheptanoic Acid (Tetrahydropyran-2-yloxy)amide (14a). A solution of **13a** (110 mg; 0.31 mmol) dissolved in CH_2Cl_2 (10 mL) was reacted with 3-phenyl-2-(phenylsulfonyl)oxaziridine (89 mg; 0.34 mmol) overnight at room temperature. The organic layer was worked up and chromatographed (*n*-hexane/AcOEt, 1:1) leaving 60 mg (52%) of a colorless foam. MS (EI): 285 $(M - THP - H)^-$. IR (MIR): 1680, 1443, 1114, 1034, 1018 cm^{-1}. ^{1}H NMR: 0.57 (t, *J* = 6, 3H); 0.75−1.75 (m, 12H); 2.85 (m, 1H); 3.45 and 4.05 (2m, 2 × 1H); 4.60 (d, *J* = 6, 1H); 4.90 (d, *J* = 5, 1H); 6.15 (t, *J* = 6, 1H); 7.61 (m, 3H); 7.79 (m, 2H); 11.2 (2s, 1H).

(f) 1:1 Mixture of (*2S,3R*)-3-[(*R*)- and (*S*)-Benzenesulfinyl]-2-hydroxyheptanoic Acid Hydroxyamide (15a). A solution of **14a** (35 mg, 0.1 mmol) dissolved in a mixture of CH_2Cl_2/MeOH/H_2O (3:2:1; 6 mL) was treated with Amberlyst IR15 (10 mg) for 3 days. The mixture was filtered and washed with MeOH. The solvents were evaporated under reduced pressure and the residue was purified by chromatography (AcOEt) leaving 18 mg (63%) of colorless powder. MS (ISN): 284.3 $(M - H)^-$. ^{1}H NMR: 0.58 (t, *J* = 6, 3H); 0.75−1.75 (m, 6H); 2.85 (m, 1H); 4.55 (dd, *J* = 2 and 5, 1H); 6.05 (d, *J* = 6, 1H); 7.61 (m, 3H); 7.79 (m, 2H); 8.77 (s, 1H); 10.7 (s, 1H).

Enzyme Inhibition. *E. coli* PDF was isolated, as recombinant enzyme from *E. coli*, in its native iron containing form and purified according to the literature method.[9] PDF activity was measured at room temperature in a microtiter plate format with 5 mM formyl-methionine-alanine-serine (f-MAS) at pH 7.2 (100 mM MOPS-KOH, 250 mM KCl, 0.4% BSA, 100 μg/mL catalase) in a total volume of 50 μL. The reaction was initiated by the addition of PDF, Fe-PDF with approximately 1100 U/mg (final concentrated: 5.7 nM), and stopped after 5 min. with 200 μL of fluorescamine. After 30 min at room temperature, the optical density was measured at 380 nm and the amount of hydrolyzed substrate determined against a standard curve of MAS which was run in parallel. Inhibitors were tested at a final concentration of 1% DMSO.

Inhibition of ACE, ECE, NEP and several matrix metalloproteases (MMP) was determined according to known literature procedures.[18−21]

In Vitro Antibacterial Activity. Bacterial strains used in this study were from our own in-house strain collection. They were obtained from the American Type Culture Collection (ATCC) and from various hospitals and kept at − 80 °C. The minimal inhibitory concentrations (MICs) of the test compounds were determined by microdilution following the guidelines of the National Committee for Clinical Laboratory Standards.[27] The MIC of a compound was defined as the lowest concentration that prevents visible growth of bacteria after incubation at 37 °C for 18−24 h. Iso-Sensitest broth (Oxoid) was used as the test medium. It was supplemented as appropriate for testing fastidious bacteria. Susceptibility of *M. pneumoniae* was tested in PPLO broth with phenol red.[28] Activity against *C. pneumoniae* was tested with cell culture of Hep-2 cells in 96-well microtiter plates.[29]

Uptake of Radiolabeled 8d and 9a in *E. coli* Cells. *E. coli* DC2 is a LPS altered outer membrane hyperpermeable mutant[23,24] of parental strain UB1005. 3-[^{14}C]-Radiolabeled **8d** and **9a** (specific activity, 11.3 and 13.0 mCi/mmol, respectively) were used for the study. Bacteria were grown to the late exponential phase at 37 °C in medium A (0.7% K_2HPO_4, 0.3% KH_2PO_4, 0.05% trisodium citrate, 0.01% $MgSO_4 \cdot 7H_2O$, 0.1% $(NH_4)_2SO_4$) supplemented with 0.2% glucose, 0.1% casamino acids, 1 μg/mL thiamine chloride, and 10 μg/mL methionine. Cells were harvested, washed twice with 50 mM of MOPS-KOH buffer (pH 6.6) and suspended to OD_{600} = 20 with the same buffer containing 0.2% glucose and 100 μg/mL chloramphenicol. Cells were vigorously shaken at 37 °C for 20 min. Uptake was started by adding 100 μL of radiolabeled compound to the same volume of cells (0.76 mg dry weight) and incubated at 30 °C. At indicated times, 3 mL of wash buffer (50 mM MOPS-KOH, pH 6.6, 5 mM citrate, and 1% DMSO) was added and cells were immediately filtered through Whatman GF/F filters. Filters were washed, dried, and counted with a liquid scintillation counter. We suggest that the washing procedure causes some leakage of the compounds which can explain the difference between the maximal equilibrium measured under uncoupling conditions and the expected calculated level. The intracellular concentration was calculated with cell volume, determined by the method reported by Rottenberg[30] as 1.55 μL/mg dry weight of cells for DC2 strain.

Structure Determination. For crystallization and X-ray structure determination, *E. coli* PDF containing nickel was used.[9] Crystals of space group *C*2 were obtained under similar conditions to what these authors used and soaked with 1 mM **8d** in 54% ammonium sulfate, 100 mM Tris, pH 8.5. Diffraction data were collected at 15 °C to 3.0 Å on an Enraf Nonius FR571 generator equipped with a graphite monochromator and a Siemens Hi-Star detector. Data were processed with the program XDS[31] and reduced with the CCP4 package.[32] The unit cell parameters were *a* = 142.91 Å, *b* = 63.90 Å, *c* = 84.44 Å, β = 123.1°. The inhibitor density, and in particular the stereochemistry, was clear from a difference map computed against a previously determined model of Ni-PDF. The inhibitor complex was refined with program CNS[33] to a final *R*-factor of 22.4% (*R*-free 26.2%) with tight geometrical constraints (rms bond errors 0.007 Å, rms angle errors 1.29°). Modeling and figure generation were performed with the in-house program Moloc.[34]

Acknowledgment. We are grateful to our colleagues from the Central Units for performing the spectroscopic measurements and for the determination of the microanalysis and our colleagues from NRRC for running the enzyme inhibition screen. We also thank Dr. Ph. Huguenin and R. Preiswerk for the synthesis of the radiolabeled compounds **8d** and **9a**; E. Bald, F. Gerber, E. Philipp, B. Prud'hon, D. Zulauf, C. Lacoste, B. Rutten, and O. Partouche for their excellent technical assistance; and Dr. H. Matile for testing antichlamydial activity. For enzyme preparation, we thank Dr. B. Takács, R. Remy, and B. Gsell. For crystal preparation, we thank M. Stihle and A. D'Arcy. We thank also D. Blum and Dr. B. Löffler for assays with ACE, ECE, and NEP and R. T. MacKenzie for determination of metalloprotease inhibition. We thank Dr. V. Wagner, University of Heidelberg, Germany, for valuable advice on enzyme preparation and properties.

Supporting Information Available: Yield of preparation and MS and NMR data of intermediates **4**−**6**. This

material is available free of charge via the Internet at http://pubs.acs.org.

References

(1) Meinnel, T.; Lazennec, C.; Villoing, S.; Blanquet, S. Structure−function relationships within the peptide deformylase family. Evidence for a conserved architecture of the active site involving three conserved motifs and a metal ion. *J. Mol. Biol.* **1997**, *267*, 749−761.

(2) Mazel, D.; Coic, E.; Blanchard, S.; Saurin, W.; Marliere, P. A survey of polypeptide deformylase function throughout the eubacterial lineage. *J. Mol. Biol.* **1997**, *266*, 939−949.

(3) Mazel, D.; Pochet, S.; Marliere, P. Genetic characterization of polypeptide deformylase a distinctive enzyme of eubacterial translation. *EMBO J.* **1994**, *13*, 914−923.

(4) Lelievre, Y.; Bouboutou, R.; Cartwright, T. Inhibition of synovial collagenase by actinonin. Structure−activity relationship. *Pathol. Biol.* **1989**, *37*, 43−46.

(5) Umezawa, H.; Aoyagi, T.; Tanaka, T.; Suda, H.; Okuyama, A.; Naganawa, H.; Hamada, M.; Takeuchi, T. Production of actinonin, an inhibitor of aminopeptidase M, by actinomycetes. *J. Antibiot.* **1985**, *38*, 1629−1630.

(6) Broughton, B. J.; Chaplen, P.; Freeman, W. A.; Warren, P. J.; Wooldridge, K.; Wright, D. E. Studies concerning the antibiotic actinonin. VIII Structure−activity relations in the actinonin series. *J. Chem. Soc., Perkin Trans. 1* **1975**, *9*, 857−860.

(7) Rajagopalan, P. T. R.; Yu, X. C.; Pei, D. Peptide deformylase, a new type of mononuclear iron protein. *J. Am. Chem. Soc.* **1997**, *119*, 12418−12419.

(8) Becker, A.; Schlichting, I.; Kabsch, W.; Schultz, S.; Wagner, A. F. V. Structure of peptide deformylase and identification of the substrate binding site. *J. Biol. Chem.* **1998**, *273*, 11413−11416.

(9) Groche, D.; Becker, A.; Schlichting, I.; Kabsch, W.; Schultz, S.; Wagner A. F. V. Isolation and crystallization of functionnally competent *Escherichia coli* peptide deformylase forms containing either iron or nickel in the active site. *Biochem. Biophys. Res. Commun.* **1998**, *246*, 342−346.

(10) Becker, A.; Schlichting, I.; Kabsch, W.; Groche, D.; Schultz, S.; Wagner A. F. V. Iron centre, substrate recognition and mechanism of peptide deformylase. *Nat. Struct. Biol.* **1998**, *5*, 1053−1058.

(11) Hao, B.; Gong, W.; Rajagopalan, R.; Zhou, Y.; Pei, D.; Chan, M. K. Structural basis for the design of antibiotics targeting peptide deformylase. *Biochemistry* **1999**, *38*, 4712−4719.

(12) Ruden, R. A. Trimethylsilylketene. Acylation and Olefination Reactions. *J. Org. Chem.* **1974**, *39*, 3607−3608.

(13) Woon, H.; Romo, D. Studies of asymmetric [2+2] cycloaddition of silylketenes and aldehydes employing Ti-TADDOL catalysts. *Tetrahedron Lett.* **1998**, *39*, 2877−2880.

(14) Davis, A. F.; Stringer, O. D. Chemistry of oxaziridines. 2. Improved synthesis of 2-sulfonyloxaziridines. *J. Org. Chem.* **1982**, *47*, 1774−1775.

(15) Wang, Z.; Zhou, W. Asymmetric epoxidation of allylic alcohol by modified Sharpless reagent. *Tetrahedron* **1987**, *43*, 2935−2944.

(16) Paddon-Jones, G.; Moore, C.; Brecknell, D.; Koenig, W.; Kitching W. Synthesis and absolute stereochemistry of Hagen's-Gland lactones in some parasitic waspes (hymenoptera: braconidae). *Tetrahedron Lett.* **1997**, *38*, 3479−3482.

(17) Oguri, T.; Shioiri, T.; Yamada, S. Amino acids and peptides. XV. New synthesis of α-amino acids by amination of α-metalated carboxylic acids. *Chem. Pharm. Bull.* **1975**, *23*, 167−172.

(18) Carmel, A.; Ehrlich-Rogozinsky, S.; Yaron, A. A fluorometric assay for angiotensin-I converting enzyme in human serum. *Clin. Chim. Acta* **1979**, *93*, 215−220.

(19) Carvalho, K. M.; Boileau, G.; Camargo, A. C. M.; Juliano, L. A highly selective assay for neutral endopeptidase based on the cleavage of a fluorogenic substrate related to Leu-enkephalin. *Anal. Biochem.* **1996**, *237*, 167−173.

(20) Schweizer, A.; Loeffler, B. M.; Rohrer, J. Palmitoylation of the three isoforms of human endothelin-converting enzyme-1. *Biochem. J.* **1999**, *340*, 649−656.

(21) Knight, C. G.; Willenbrock, F.; Murphy, G. A novel coumarin-labeled peptide for sensitive continuous assays of the matrix metalloproteinases. *FEBS Lett.* **1992**, *296*, 263−266.

(22) Apfel, C. Manuscript in preparation.

(23) Richmond, M. H.; Clark, D. C.; Wotton, S. Indirect method for assessing the penetration of β-lactamase-nonsusceptible penicillins and cephalosporins in *Escherichia coli* strains. *Antimicrob. Agents Chemother.* **1976**, *10*, 215−218.

(24) Rocque, W. J.; Fesik, S. W.; Haug, A.; McGroarty, E. J. Polycation binding to isolated lipopolysaccharide from antibiotic-hypersusceptible mutant strains of *Escherichia coli*. *Antimicrob. Agents Chemother.* **1988**, *32*, 308−313.

(25) Margolis, P.; Hackbarth, C.; White, R.; Lopez, S.; Trias, J. Resistance to deformylase inhibitor VRC483 is caused by mutations in formylase transferase. 39th Annual ICAAC Meeting, San Francisco, CA, 1999; Abstract No. 1795, Book of Abstracts, 334.

(26) Newton, D. T.; Creuzenet, C.; Mangroo D. Formylation is not essential for initiation of protein synthesis in all eubacteria. *J. Biol. Chem.* **1999**, *274*, 22143−22146.

(27) National Committee for Clinical Laboratory Standards. *Methods for dilution antimicrobial susceptibility tests for bacteria that grow aerobically*, 3rd ed.; National Committee for Clinical Laboratory Standards: Villanova, PA, 1993; Vol. 13, No. 25, M7-A3.

(28) Kaku, M.; Ishida, K.; Irifune, K.; Mizukane, R.; Takemura, H.; Yoshida, R.; Tanaka, H.; Usui, T.; Tomono, K.; Suyama, N.; Koga, H.; Kohno, S.; Hara, K. In vitro and in vivo activities of sparfloxacin against *Mycoplasma pneumoniae*. *Antimicrob. Agents Chemother.* **1994**, *38*, 738−741.

(29) Roblin, P. M.; Montalban, G.; Hammerschlag, M. R. Susceptibilities to clarithromycin and erythromycin of isolates of *Chlamydia pneumoniae* from children with pneumonia. *Antimicrob. Agents Chemother.* **1994**, *38*, 1588−1589.

(30) Rottenberg, H. Proton electrochemical potential gradient in vesicles, organelles, and prokaryotic cells. *Methods Enzymol.* **1989**, *172*, 63−84.

(31) Kabsch, W. Evaluation of single-crystal X-ray diffraction data from a position-sensitive detector. *J. Appl. Crystallogr.* **1988**, *21*, 916−924.

(32) Bailey, S. Collaborative Computational Project, Number 4. The CCP4 suite: programs for protein crystallography. *Acta Crystallogr.* **1994**, *D50*, 760−763.

(33) Brünger, A. T.; Adams, P. D.; Clore, G. M.; DeLano, W. L.; Gros, P.; Grosse-Kunstleve, R. W.; Jiang, J.-S.; Kuszewski, J.; Nilges, M.; Pannu, N. S.; Read, R. J.; Rice, L. M.; Simonson, T.; Warren, G. L. Crystallography and NMR system: a new software suite for macromolecular structure determination. *Acta Crystallogr.* **1998**, *D54*, 905−921.

(34) Gerber, P. R.; Müller, K. MAB: A generally applicable molecular force field for structure modelling in medicinal chemistry. *J. Comput.-Aided Mol. Des.* **1995**, *9*, 251−268.

JM000018K